

## NICMOS Imaging of Damped Ly- $\alpha$ Absorbers at $z = 2$

Varsha P. Kulkarni<sup>1</sup>, John M. Hill, Glenn Schneider,  
*Steward Observatory, University of Arizona, Tucson, AZ 85721*

Ray J. Weymann, Lisa J. Storrie-Lombardi  
*Carnegie Observatories, Pasadena, CA 91101*

Marcia J. Rieke, Rodger I. Thompson,  
*Steward Observatory, University of Arizona, Tucson, AZ 85721*

Buell Jannuzi  
*National Optical Astronomy Observatories, Tucson, AZ 85726*

**Abstract.** We report results from deep NICMOS imaging of the fields of two damped Lyman- $\alpha$  (DLA) quasar absorbers at  $z_{DLA} = 1.89$  and  $z_{DLA} = 1.86$ . The images were obtained in the broad filter F160W and the narrow filter F190N or F187N with camera 2 on NICMOS, with the goal of detecting the rest-frame optical continuum and H- $\alpha$  emission from the DLA absorbers. The broad band images put sensitive constraints on the sizes of the DLAs, while the narrow band images put the tightest existing limits on the star formation rates in DLAs. These results have important implications for the physical nature of DLA absorbers.

### 1. Introduction

Damped Lyman-alpha (DLA) absorbers in spectra of high-redshift quasars are believed to trace the precursors of present-day galaxies. But the nature of absorbing galaxies is not yet understood. DLAs have been variously thought to arise in large rotating proto-disks (e.g., Wolfe et al. 1986, Prochaska & Wolfe 1997) or dwarf galaxies (e.g., York et al. 1986, Matteucci et al. 1997). Unfortunately, most previous efforts to directly image the objects causing high- $z$  DLAs have been unsuccessful. Most of these previous searches attempted to detect the redshifted Ly- $\alpha$  emission from the DLAs. However, these nondetections cannot directly constrain the star formation rate (SFR) in DLAs, since the Ly- $\alpha$  line can easily get extinguished by even small amounts of dust, owing to resonant scattering. Here we report HST NICMOS observations of the fields of the DLAs toward LBQS 1210+1731 ( $z_{DLA} = 1.892$ ,  $z_{QSO} = 2.543$ ) and

---

<sup>1</sup>Current Address: Clemson University, Dept. of Physics and Astronomy, Clemson, SC 29634

Q1244+3443 ( $z_{DLA} = 1.859$ ,  $z_{QSO} = 2.48$ ), aimed at detecting redshifted H- $\alpha$  and optical continuum emission from the DLAs.

## 2. Observations, Data Reduction, PSF Subtraction

Broad band images were obtained with NICMOS camera 2, using filter F160W ( $\lambda_{central} = 1.5940 \mu\text{m}$ , FWHM =  $0.4030 \mu\text{m}$ ), dithered in steps of 7.5 pixels. Narrow band images were also obtained using dither steps of 7.5 pixels, in filter F190N ( $\lambda_{central} = 1.9005 \mu\text{m}$ , FWHM =  $0.0174 \mu\text{m}$ ) for LBQS 1210+1731 and in filter F187N ( $\lambda_{central} = 1.8740 \mu\text{m}$ , FWHM =  $0.0192 \mu\text{m}$ ) for Q1244+3443. These filters should contain the redshifted H- $\alpha$  lines at  $z = 1.892$  and  $z = 1.859$ , respectively. Finally, coronagraphic F160W images were also obtained for each QSO (See Kulkarni et al. 1999a, 1999b). Data were reduced using the IRAF package Nired 1.8 (McLeod 1997). Reference PSFs for quasar PSF subtraction were obtained from observations of stars in the same filter / aperture combinations. The PSF star images were chosen to match as closely as possible the telescope “breathing” focus values for our quasar observations. For the coronagraphic images, more importance was given to getting close match between the exact positions in the coronagraphic hole where the quasar and the PSF star were located. The PSF star observations were analyzed in exactly the same manner as the quasar observations. The reduced PSF stars were registered and scaled to match the quasar and then subtracted from the quasar.

## 3. Searching for the DLA near LBQS 1210+1731

### 3.1. Non-coronagraphic F160W and F190N images

About 99 % of the flux in the non-coronagraphic F160W and F190N images comes from the quasar point source and disappears after PSF subtraction. A feature to the “lower right” of the center at about  $0.26''$  from the quasar (“O1”) is the main asymmetric residual left behind in the images (Fig. 1). We have carried out several tests to determine whether O1 is real or an artifact arising from HST breathing, color differences between quasar and PSF star, differences in focus settings, asymmetries in the PSF core etc. (Kulkarni et al. 1999a). The best-fitting PSF and several others with reasonably close breathing values suggest that O1 is real, given the significant excess over a number of pixels. We cannot completely rule out that O1 is some artifact arising for reasons we have not been able to account for. If O1 is associated with the DLA, then it is  $2.4 h_{0.7}^{-1}$  kpc long for  $q_0 = 0.5$  or  $3.2 h_{0.7}^{-1}$  kpc long for  $q_0 = 0.1$ . O1 has a flux of  $9.8 \pm 2.4 \mu\text{Jy}$  in the F160W filter and  $10.6 \pm 1.5 \mu\text{Jy}$  in the F190N filter. On estimating the continuum contribution to the F190N flux, there is no evidence for statistically significant redshifted H- $\alpha$  line flux. Given the low dust-to-gas ratios inferred for DLAs (e.g. Pei et al. 1991; Pettini et al. 1997 and references therein), the nondetection of H- $\alpha$  emission is likely to be because of low SFR. Assuming no dust and using the H- $\alpha$  luminosity-SFR conversion of Kennicutt (1983), the  $3\sigma$  upper limit on the SFR is  $4.0 h_{0.7}^{-2} M_{\odot} \text{yr}^{-1}$  for  $q_0 = 0.5$ . This is the tightest existing constraint on the SFR in DLAs.

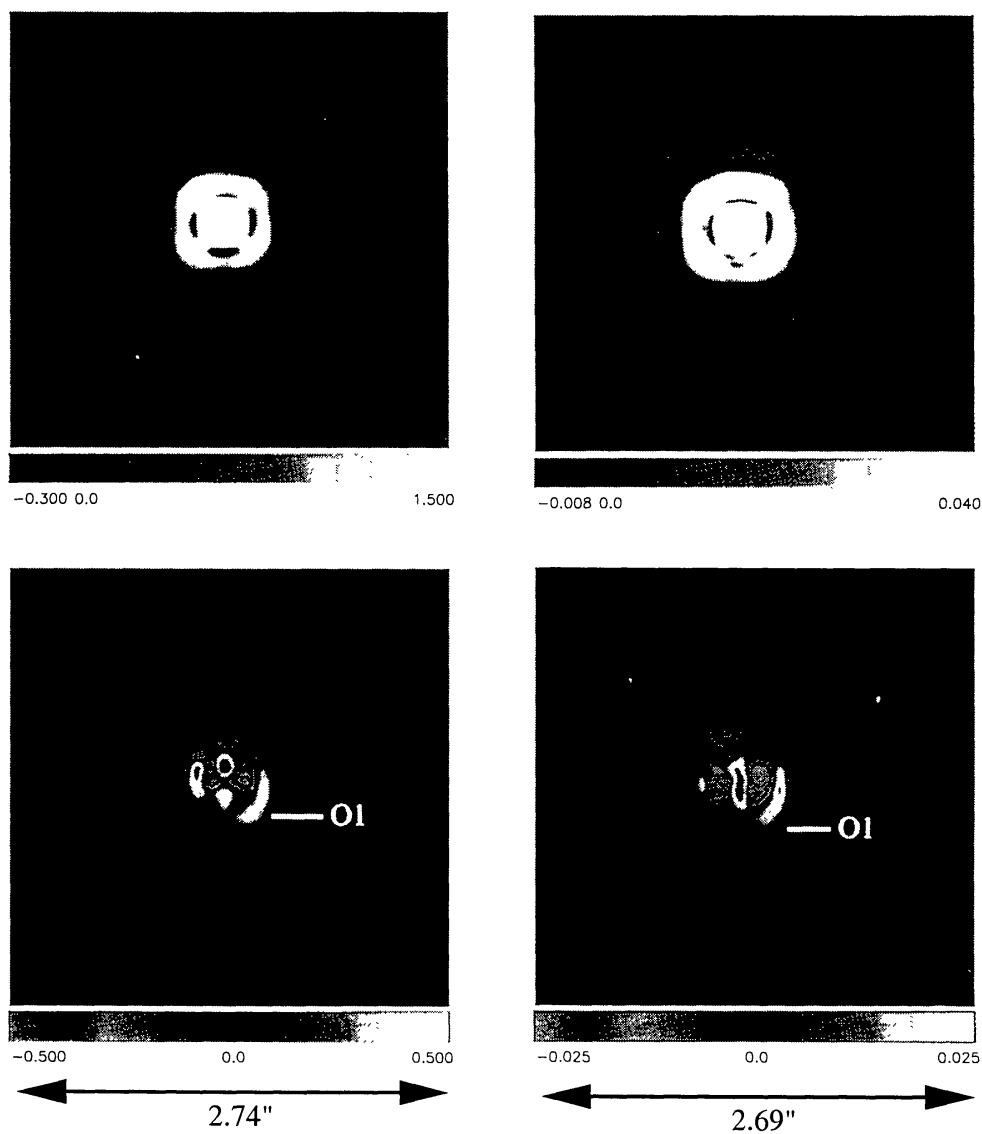


Figure 1. Left: Zoomed-in  $2.74'' \times 2.71''$  region of the NICMOS camera 2 non-coronagraphic  $1.6 \mu\text{m}$  broad-band image of Q1210+1731, (a) before (top) and (b) after (bottom) PSF subtraction (bottom). Right: Zoomed-in  $2.69'' \times 2.66''$  region of the NICMOS camera 2 non-coronagraphic  $1.9 \mu\text{m}$  narrow-band image of Q1210+1731, (c) before (top) and (d) after (bottom) PSF subtraction.

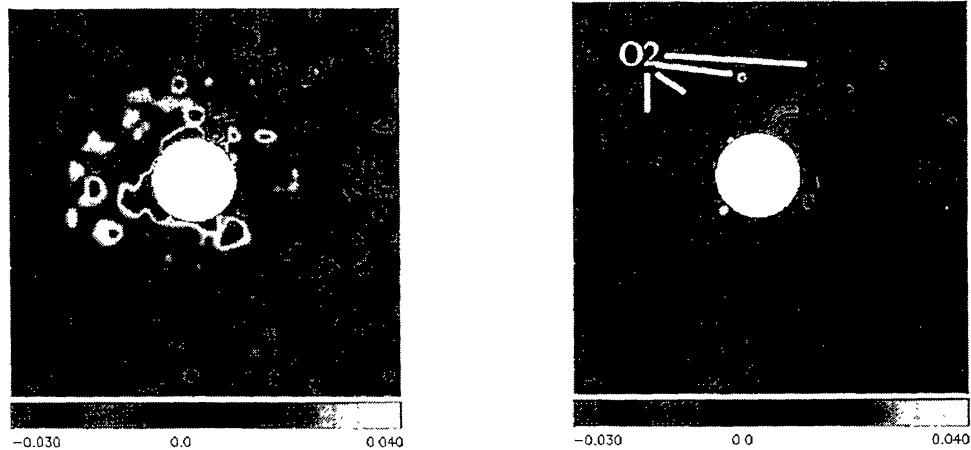


Figure 2. Zoomed-in  $2.89'' \times 2.81''$  regions of coronagraphic  $1.6 \mu\text{m}$  image of Q1210+1731, (a) before (left) and (b) after (right) PSF subtraction

### 3.2. Coronagraphic Image of LBQS1210+1731

The NICMOS coronagraph reduces the scattered and diffracted energy from the occulted target's PSF core by factors of 4-6, compared to direct imaging (Schneider et al. 1998; Lowrance et al. 1998). Most of the flux in the coronagraphic images comes from small amount of scattered light from the quasar and glints from the edge of the hole. These disappear almost completely after PSF subtraction. But a weak feature consisting of several knots (object "O2") remains at about  $0.7''$  from the quasar center (Fig. 2). There are no known artifacts in the coronagraphic F160W image at the positions of the O2 knots. If O2 is at the redshift of the DLA, it has a total size of  $4-5 h_{0.7}^{-1} \text{ kpc}$  for  $q_0 = 0.5$ .

## 4. The DLA toward Q1244+3443

The results for this DLA are similar to those for the DLA toward Q1210+1731 (Fig. 3). Note the possible presence of a compact object below the quasar center in the F160W image, at a separation of only  $0.16''$ . The narrow-band image reveals no strong extended emission from this or any other source, suggesting a low SFR. Further details are discussed by Kulkarni et al. (1999b). Thus, our observations of both the DLAs suggest compact or low surface brightness objects with a few continuum emission knots, and low star formation rates.

**Acknowledgments.** This work was supported by NASA grant NAG5-3042.

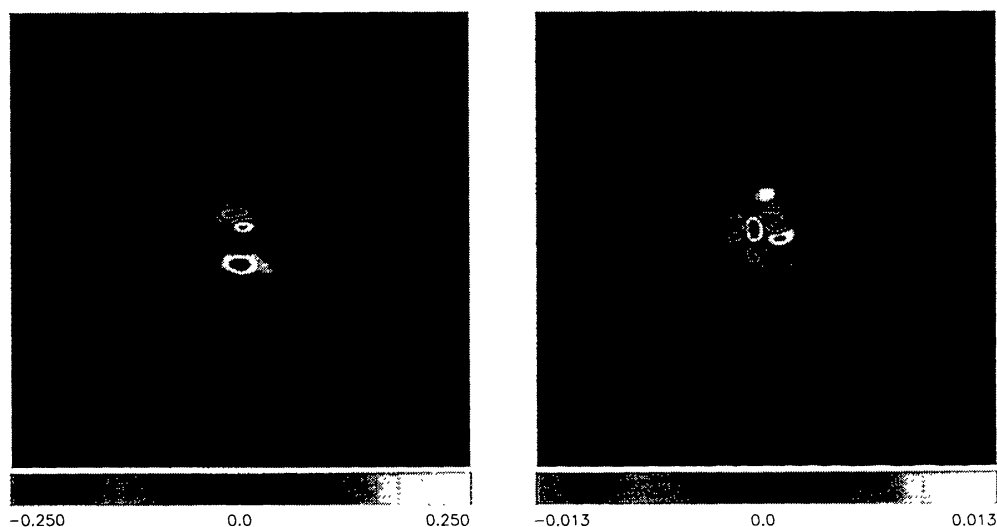


Figure 3. Zoomed-in  $2.81'' \times 2.79''$  regions of the NICMOS camera 2 non-coronagraphic (a)  $1.6 \mu\text{m}$  (left) and (b)  $1.87 \mu\text{m}$  (right) images of the field of Q1244+3443, after PSF subtraction

## References

- Kennicutt, R. C. 1983, *ApJ*, 272, 54
- Kulkarni, V. P., Hill, J. M., Schneider, G., Weymann, R. J., Storrie-Lombardi, L. J., Rieke, M. J., Thompson, R. I., & Jannuzi, B. 1999a, *ApJ*, submitted
- Kulkarni, V. P., Hill, J. M., Schneider, G., Weymann, R. J., Storrie-Lombardi, L. J., Rieke, M. J., Thompson, R. I., & Jannuzi, B. 1999b, in preparation
- Lowrance, P. et al. 1998, in Proc. 'NICMOS and the VLT' (ESO), 96
- Matteucci, F., Molaro, P., & Vladilo, G. 1997, *A&A*, 321, 45
- McLeod, B. 1997, in Proc. 1997 HST Calibration Workshop, eds. S. Casertano et al. (STScI), 281
- Pei, Y. C., & Fall, S. M. 1995, *ApJ*, 454, 69
- Prochaska, J. X., & Wolfe, A. M. 1997, *ApJ*, 487, 73
- Pettini, M., King, D. L., Smith, L. J., & Hunstead, R. W. 1997, *ApJ*, 478, 536
- Schneider, G., Thompson, R. I., Smith, B. A., & Terrile, R. J. 1998, *SPIE Conf. Proc. Ser.*, 3356
- Wolfe, A. M., Turnshek, D. A., Smith, L. J., Cohen, R. D. 1986, *ApJS*, 61, 249
- York, D. G., Dopita, M., Green, R., & Bechtold, J. 1986, *ApJ*, 311, 610